Exciton–Polaron-Induced Aggregation of Wide-Bandgap Materials and its Implication on the Electroluminescence Stability of Phosphorescent Organic Light-Emitting Devices

*Qi Wang, Bin Sun, and Hany Aziz**

The degradation mechanisms of phosphorescent organic light-emitting devices (PhOLEDs) are studied. The results show that PhOLED degradation is closely linked to interactions between excitons and positive polarons in the host material of the emitter layer (EML), which lead to its aggregation near the EML/electron transport layer (ETL) interface. This exciton–polaron-induced aggregation (EPIA) is associated with the emergence of new emission bands at longer wavelengths in the electroluminescence spectra of these materials, which can be detected after prolonged device operation. Such EPIA processes are found to occur in a variety of wide-bandgap materials commonly used as hosts in PhOLEDs and are correlated with device degradation. Quite notably, the extent of EPIA appears to correlate with the material's bandgap rather than with the glass-transition temperature. The findings uncover a new degradation mechanism, caused by polaron-exciton interactions, that appears to be behind the lower stability of OLEDs utilizing wide-bandgap materials in general. The same degradation mechanism can be expected to be present in other organic optoelectronic devices.

1. Introduction

Organic light-emitting devices (OLEDs) are emerging as the next generation technology for flat panel displays and solid-state lighting because of their advantages in realizing low-cost, large-size and mechanically flexible applications. Phosphorescent OLEDs (PhOLEDs), employing heavy-metal organometallic emitter molecules doped into wide-bandgap host materials, have particularly attracted tremendous attention due to their unique capability in achieving device internal quantum efficiency nearly 100%.[1–5] However, these highly efficient devices have relatively poor electroluminescence (EL) stability compared to their fluorescent counterparts,[6] which significantly limits their commercialization. Understanding the degradation behavior of PhOLEDs has therefore been the focus of a significant number of studies,[7–13] leading to the identification of several degradation mechanisms. These mechanisms include annihilation reactions between host anions and guest excitons,[7,8] homolytic cleavage of C-N bonds in host molecules when in the excited state,[9] molecular dissociation of hole-blocking and electron-blocking materials,[10] and buildup of hole space charges in light-emitting layers.[11–13]

Despite identifying various degradation mechanisms, these studies have primarily focused on degradation phenomena that occur in bulk organic materials. The role of device interfaces in limiting device EL stability has received attention only recently. For example, we recently found that the interface between indium tin oxide (ITO) and organic materials is susceptible to degradation by excitons,[14] and that the phenomenon plays a role in limiting the stability of the simplified PhOLEDs.[15] More recently we found that the interface between the emitter layer (EML), which typically employs a wide-bandgap host material (HM), and the electron transport layer (ETL) is also susceptible to degradation by excitons, but in this case when charges are also present in the vicinity of the interface.[16] This degradation process leads to a deterioration in conduction across the interfaces and contributes to the increase in device driving voltage (V_d) commonly observed with continuous electrical driving time.[16] Aside from being interfacial, and thus arises from processes that are different from those behind the aforementioned bulk degradation mechanisms, the finding has highlighted the fact that the combined effect of excitons and polarons on PhOLED stability can be quite different from their effects individually, in line with the observations by Giebink et al.[7,8] Different from those observations, however, which were attributed to interactions between host anions and guest excitons in bulk materials,[7,8] this interfacial degradation is induced by interactions between excitons and positive polarons on HMs. The underlying mechanism by which such interaction results in a permanent EL efficiency loss in the devices has however remained

Q. Wang, Prof. H. Aziz
Department of Electrical & Computer Engineering
and Waterloo Institute for Nanotechnology
University of Waterloo
200 University Avenue West
Waterloo, Ontario, N2L 3G1, Canada
E-mail: h2aziz@uwaterloo.ca
B. Sun
Department of Chemical Engineering
University of Waterloo
200 University Avenue West
Waterloo, Ontario, N2L 3G1, Canada

DOI: 10.1002/adfm.201303840

unclear. Furthermore, given the critical role of HM exctions in exciton-polaron interactions, it is natural to wonder if PhOLEDs employing wide-bandgap HMs, and thus have high-energy excitons on HMs during normal device operation, are more susceptible to this degradation behavior, and whether it is the use of wide-bandgap HMs in PhOLEDs that essentially makes them much less stable than their fluorescent counterparts which usually do not contain wide-bandgap materials.

In this study, we investigate the degradation mechanisms of EML/ETL interfaces in PhOLEDs. 4,4′-Bis(carbazol-9-yl) biphenyl (CBP)/1,3,5-tris(*N*-phenyl-benzimidazol-2-yl)-benzene (TPBi) interface is studied as a typical EML/ETL interface because of its widespread use in highly efficient PhOLEDs.[3] The results show that the CBP/TPBi interface degrades significantly when both CBP excitons and CBP positive polarons are present simultaneously in their vicinity. Such interfacial degradation is found to be associated with a change in device EL spectrum, due to the emergence of a new band at ~500 nm. The new band is determined to arise from CBP aggregation which occurs in the vicinity of the CBP/TPBi interface. This molecular aggregation is not unlike what occurs in anthracene-based fluorescent OLEDs.[17] Further investigations reveal that the CBP aggregation process in PhOLEDs is essentially induced by interactions between CBP excitons and CBP positive polarons at the CBP/TPBi interface. Finally, similar exciton-polaron-induced aggregation behavior is verified to occur in a range of wide-bandgap materials, and it plays a primary role in the EL stability of PhOLEDs.

2. Results and Discussion

2.1. PhOLEDs Degradation due to Exciton-Polaron Interactions

We first study the degradation behavior of CBP/TPBi-based PhOLEDs, in which fac-tris(2-phenylpyridine) iridium ($Ir(ppy)_3$) is used as the phosphorescent emitter material doped into the CBP host in various concentrations. The general structure of the devices is ITO/MoO_3(5 nm)/CBP(30 nm)/CBP:$Ir(ppy)_3$(10 nm)/TPBi(30 nm)/LiF(0.5 nm)/Al(100 nm), as shown in **Figure 1**a. The $Ir(ppy)_3$ concentration in these devices is 0, 0.1%, 1% or 4%. Figure 1b shows the changes in V_d (ΔV, defined as the V_d at any given time minus the initial V_d) and EL intensity (normalized to initial values) of the devices versus time during which the devices are continuously driven by a current of density 20 mA cm^{-2}. The initial brightness values of the devices with 0, 0.1%, 1% and 4% $Ir(ppy)_3$ are 50, 2000, 7800 and 7500 cd m^{-2}, respectively. The initial V_d values of these devices are 6.8, 7.3, 7.6 and 7.7 V, respectively. As the figure shows, an increase in $Ir(ppy)_3$ concentration leads to more stable EL and V_d with time. For example, the lifetime (defined as the time elapsed before the EL decreases to 50% of its initial value) of the devices with 0, 0.1%, 1%, and 4% $Ir(ppy)_3$ is ~0.2, 0.5, 8, and 19 h, respectively. Such trend cannot be explained by the previously proposed mechanisms that attribute degradation primarily to excitons on guest molecules (i.e., $Ir(ppy)_3$ triplets in this case),[7,8] since clearly the device with 0.1% $Ir(ppy)_3$ degrades much faster than those with 1% and 4% $Ir(ppy)_3$, despite the lower concentration of $Ir(ppy)_3$ triplets. The trend also contradicts the commonly accepted notion that the lifetime of a PhOLED is inversely proportional to its initial brightness.[18] Figure 1c shows normalized EL spectra of these devices. As expected, the devices with higher $Ir(ppy)_3$ concentration show less EL from CBP (i.e., the band at ~ 400 nm), an observation that can be attributed to the more efficient energy transfer from the host to guest molecules via Forster process as the guest concentration increases. A comparison of the results in Figure 1(b) and (c) suggests there may be a correlation between the lower device stability of the devices with lower $Ir(ppy)_3$ concentrations and the higher ratio of CBP to $Ir(ppy)_3$ excitons in them.

To verify this, we study the time-resolved photoluminescence (PL) of both CBP and $Ir(ppy)_3$ in CBP:$Ir(ppy)_3$ films with different $Ir(ppy)_3$ concentrations. **Figure 2**a and b show luminescence decay in time at 400 nm and 520 nm (i.e., from the relaxation of CBP singlet excitons and $Ir(ppy)_3$ triplet excitons), respectively, collected from CBP:$Ir(ppy)_3$ films (~30 nm thick, deposited on a quartz substrate) with 0%, 0.1%, 1% and 4% $Ir(ppy)_3$ following excitation at 379 nm using a laser pulse (pulse width ~71 ps, average power ~5 mW). As Figure 2a shows, the decay rate of CBP fluorescence becomes faster as $Ir(ppy)_3$ concentration increases. That the CBP fluorescence decay rates in the samples with 1% and 4% $Ir(ppy)_3$ are similar in Figure 2a can be attributed to the very fast decay rate in both cases, which makes the rate approach the fall time of the laser excitation pulse itself as seen from the overlap in the curves. On the other hand, as can be seen in Figure 2b, the decay rate of $Ir(ppy)_3$ phosphorescence remains almost the same for the various $Ir(ppy)_3$ concentrations. The increase in CBP fluorescence decay as $Ir(ppy)_3$ concentration increases is indicative of a more efficient quenching of CBP excitons by $Ir(ppy)_3$ via Forster process. It follows that in PhOLEDs with higher $Ir(ppy)_3$ concentration the CBP excitons produced by electron-hole (e-h) recombination during device operation will also have shorter lifetime in comparison to in devices with lower $Ir(ppy)_3$ concentration. Therefore, in these devices, the number of CBP excitons present at any point in time will be smaller, which is also consistent with the observation that the EL from CBP in these devices is negligible. Such CBP-exciton dependence of PhOLEDs degradation, however, does not necessarily mean that the degradation process is simply caused by the presence of CBP excitons. We have in fact determined that the presence of CBP excitons alone leads to very little degradation in bulk organic materials. On the other hand, the simultaneous presence of both CBP excitons and CBP positive polarons can cause significant degradation of the CBP/TPBi interface via exciton-polaron interactions.[16] Since the concentration of CBP positive polarons at the CBP/TPBi interface can be expected to be comparable in all devices in Figure 1, whereas the lifetime of CBP excitons is much shorter in the devices with higher $Ir(ppy)_3$ concentration, the degradation process will be slower in the devices with higher $Ir(ppy)_3$ concentration due to the shorter CBP exciton lifetime, and thus a lower probability for exciton-polaron interactions. This is precisely the trend shown in Figure 1. Therefore, the results in Figure 1 and 2 are consistent with our recent findings that CBP excitons contribute to device degradation through their interactions with CBP positive polarons at the CBP/TPBi interface.[16]

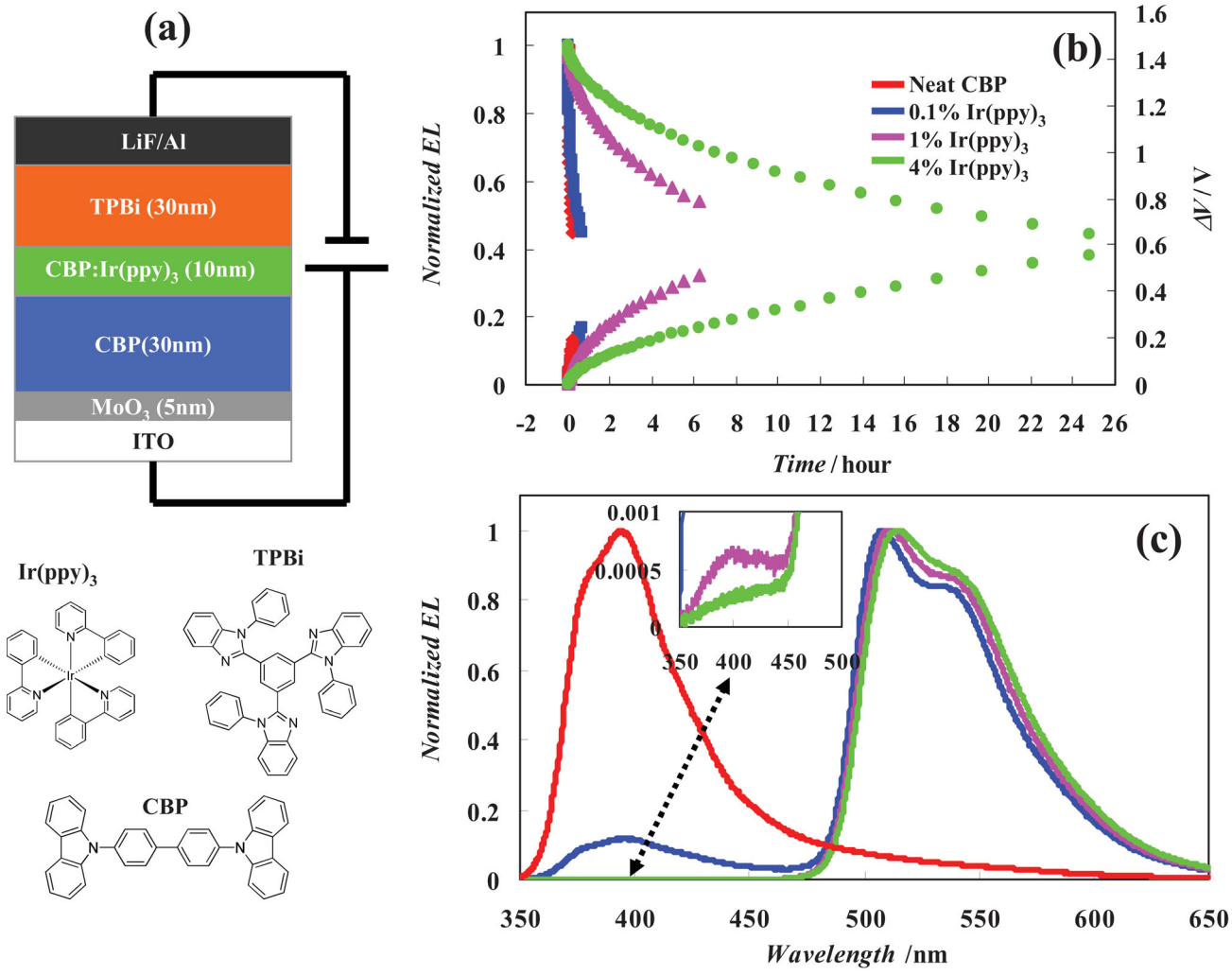

Figure 1. (a) Structure of PhOLEDs and molecular structures of the materials used. (b) Changes in normalized EL and V_d of the devices with different $Ir(ppy)_3$ concentrations versus time during which the devices are continuously driven by a current of density 20 mA cm^{-2}. (c) Normalized EL spectra of the devices. The inset of (c) shows a detailed view of the spectra in the short-wavelength region.

2.2. Electrical-Driving-Induced CBP Aggregation

In order to obtain more insights into the mechanism by which interactions between excitons and polarons on CBP lead to device degradation, we study a device with a neat CBP emitting layer. **Figure 3**a and b show EL spectra (with and without normalization, respectively) with continuous electrical driving at 20 mA cm^{-2} in a CBP/TPBi-based test-device of structure ITO/MoO_3(5 nm)/CBP(40 nm)/TPBi(30 nm)/LiF(0.5 nm)/Al(100 nm). As the figures show, the device initially (at t = 0) produces blue EL from CBP with a band at ~400 nm. With time, the EL spectrum gradually broadens and a new band with a peak at ~500 nm appears. The photographs in Figure 3b depict the emission colors and corresponding CIE coordinates of the device before and after the electrical driving. Since the 500 nm band in the EL spectrum does not correspond to emission from either CBP or TPBi singlets (whose emission bands are at ~400 nm), its appearance is indicative of the formation of some new luminescent species as a result of the prolonged electrical driving. Figure 3c shows normalized PL spectra of the same device before and after the electrical stress. The spectra are collected under excitation by a 365 nm illumination with a power density of ~0.5 mW cm^{-2}. As TPBi absorbs negligibly little at this wavelength, the spectra represent PL from the CBP layer.[16] As can been seen in the figure, the PL spectra show no changes due to the electrical stress, except for a very small spectral broadening at ~500 nm. Since the EL originates primarily from the e-h recombination zone (i.e., the vicinity of the CBP/TPBi interface) whereas the PL originates from the entire CBP layer, the stark difference between the extent of changes in the EL and PL spectra suggests that the formation of the new luminescent species is limited mainly to the vicinity of the CBP/TPBi interface, where the density of both excitons and polarons is typically much higher. As TPBi can diffuse easily into HMs during device electrical driving, the EL spectral shift may be due to emission from certain CBP-TPBi exiplex species, resulting

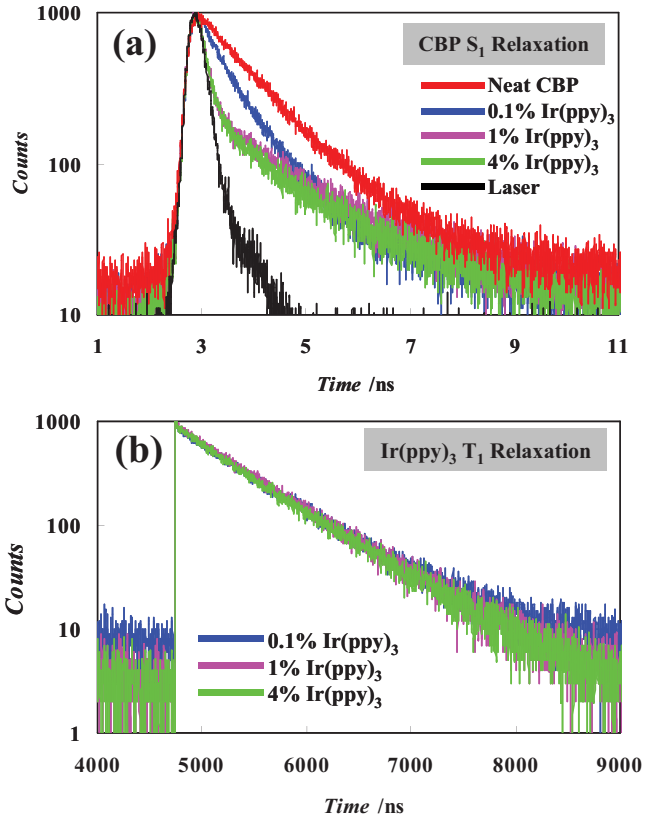

Figure 2. Luminescence decay in time (a) at 400 nm (i.e., from the relaxation of CBP singlet excitons) and (b) at 520 nm (i.e., from the relaxation of Ir(ppy)$_3$ triplet excitons) collected from CBP:Ir(ppy)$_3$ films with different Ir(ppy)$_3$ concentrations.

from the intermixing of the two materials. To investigate this possibility, we fabricate a device containing a mixed layer of CBP and TPBi in order to test if simply mixing the two materials could result in a similar red-shift. The EL spectrum from the device does not however show any new long-wavelength band and is generally identical to that of the one without the mixed layer before the stress, ruling out the possibility that the new luminescent species may arise from CBP-TPBi exciplex.

It is important to point out that the changes in EL spectra with electrical stress can be observed not only in devices with neat CBP, but also in regular devices where CBP is doped with a phosphorescent guest. Although obviously they will be difficult to detect in devices containing green-emitting dopants due to the spectral overlap between the dopants emission and this new band, they can be detected in devices with dopants emitting in the red range. **Figure 4** shows normalized EL spectra with continuous electrical driving at 20 mA cm^{-2} in a PhOLED containing the red phosphorescent emitter platinum octaethylporphine (PtOEP) of structure ITO/MoO_3(5 nm)/CBP(20 nm)/CBP:PtOEP(2%)(20 nm)/TPBi(30 nm)/LiF(0.5 nm)/Al(100 nm). As the figure shows, the device initially (at t = 0) produces a predominant amount of red EL from PtOEP triplets at ~650 nm, a small amount of blue EL from CBP singlets at ~400 nm and an extremely small amount of EL from a hot level of thermally populated PtOEP triplet states with the little spike at ~545 nm.[19] After 10 h of electrical driving, a new band at ~500 nm which precisely coincides with that in Figure 3 appears, pointing to the formation of the same new luminescent species.

From the above results, we can draw the conclusion that electrical driving results in EL spectral changes in CBP/TPBi based PhOLEDs, associated with the emergence of a new band at ~500 nm and independent of the guest materials. The reason that this phenomenon was never specifically reported in the past may be due to the difficulty in isolating this band in PhOLEDs containing green and blue emitters, due to the significant overlap in the EL spectra of these emitters and the new luminescent species. Since in these devices the majority of

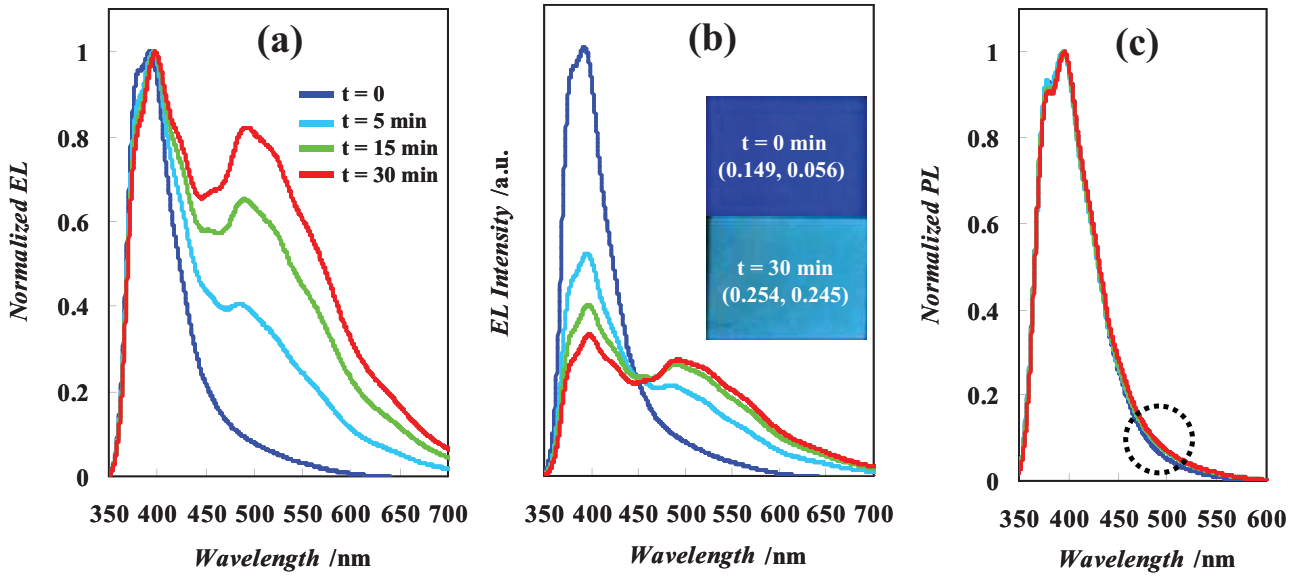

Figure 3. (a) EL (with normalization), (b) EL (without normalization) and (c) PL (with normalization) spectra with continuous electrical driving at 20 mA cm^{-2} in a device of structure ITO/MoO_3(5 nm)/CBP(30 nm)/TPBi(20 nm)/LiF(0.5 nm)/Al(100 nm). Two photographs depicting the emission colors and corresponding CIE coordinates of the device before and after electrical driving are included in (b).

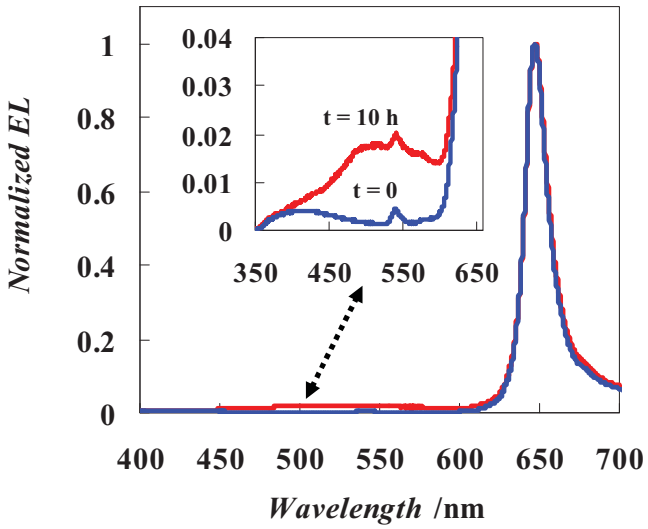

Figure 4. Normalized EL spectra of a device of structure ITO/MoO_3(5nm)/CBP(20nm)/CBP:PtOEP(2%)(20nm)/TPBi-(30nm)/LiF(0.5nm)/Al(100 nm) before and after 10 h of electrical driving at 20 mA cm^{-2}. The inset shows a detailed view of the spectra in the short-wavelength region.

e-h recombination and exciton formation occurs on CBP molecules, rather than on TPBi or $Ir(ppy)_3$ molecules directly,[11] and takes place in the vicinity of the CBP/TPBi interface, it is entirely possible that the new luminescent species may be associated with or resulting from degraded CBP molecules near the interface.

The changes in EL spectra with electrical driving time, as a phenomenon, is known to occur in blue fluorescent OLEDs, and causes the loss in color purity in these devices with electrical aging in general. Our previous studies on anthracene-based blue fluorescent OLEDs uncovered that the effect is due to the formation of anthracene aggregates, which have a lower bandgap than the monomers and hence a longer wavelength.[17] Seeing a similar effect in CBP-based devices, we wonder if a similar aggregation process, induced by electrical driving, occurs.

To test for this, we begin with investigating changes in EL spectra of CBP/TPBi-based devices due to thermal annealing. **Figure 5**a shows normalized EL spectra of a device of structure ITO/MoO_3(5 nm)/CBP(40 nm)/TPBi(30 nm)/LiF(0.5 nm)/Al(100 nm) before and after annealing at 120 °C for 20 and 60 min in a N_2 atmosphere. As the figure shows, the initial (before annealing) EL spectrum corresponds to the typical CBP emission and is identical to that in Figure 3a. After 20 min of annealing, the spectrum shows slight broadening in the long-wavelength tail. This broadening becomes significant after 60 minutes of annealing. To better illustrate the changes, the differences between the EL spectra after 20 and 60 min of annealing relative to the initial one are shown in the inset of the figure. The differences clearly correspond to a new band with a peak at ~500 nm. Quite remarkably, the changes in the EL spectra here induced by annealing are very similar to those induced by electrical driving in Figure 3 (i.e., both correspond to a new band at ~500 nm), suggesting that the new luminescent species in both cases is likely the same. Since organic molecules in general tend to aggregate under thermal annealing to increase molecular ordering, it is possible that the new emission band may be due to CBP and/or TPBi aggregates.

To understand the origin of the new luminescent species, we further study the effect of thermal annealing on the changes in PL spectra of CBP and TPBi films independently. Figure 5b shows normalized PL spectra under a 365 nm excitation of the CBP sample before and after annealing at 120 °C for 20, 60, and 100 min in a N_2 atmosphere. As the figure shows, the sample initially produces a PL spectrum of an amorphous CBP film. As the CBP sample is annealed over a period of 100 min, the PL spectrum starts to show increasingly distinguishable bands in the region of 350–450 nm. These bands can be attributed to the vibrational modes of CBP molecules, becoming increasingly resolvable as the film morphology changes gradually, by the annealing process, from an amorphous to a more crystalline one.[20] What is also shown in Figure 5b is the PL spectral broadening in the 450–650 nm region after 60 and 100 min of annealing. The differences between the PL spectra after 60 min and 100 minutes of annealing relative to the initial one are shown in the inset, again showing the emergence of a band with a peak at ~500 nm. Since the 500 nm band can be induced by just annealing, it is very likely that the new luminescent species is simply CBP aggregates. This is further verified by comparing the absorption spectra of the CBP film before and after the thermal annealing shown in Figure 5c. As the figure shows, the absorption spectrum of the annealed film shows a significant red-shift in the 300–400 nm region in comparison to that before annealing, which is consistent with the increased crystallinity (i.e., aggregation) in the bulk CBP film. Figure 5d, on the other hand, shows normalized PL spectra under a 312 nm excitation of the TPBi sample due to thermal annealing at 150 °C in a N_2 atmosphere. Unlike CBP, TPBi shows no detectable changes in the PL spectra upon annealing for the same period of time, suggesting that TPBi is not as easily susceptible to aggregation.

The results convincingly prove that the emergence of the new 500 nm band in the EL spectra due to electrical driving arise essentially from CBP aggregation. It is worthwhile to point out that such aggregation process occurs primarily in the e-h recombination zone (i.e., near the CBP/TPBi interface), and not in the entire CBP layer, since the EL spectrum changes significantly whereas the PL spectrum changes negligibly as noted earlier in Figure 3.

2.3. CBP Aggregation due to Exciton-Polaron Interactions

Although the results above show the occurrence of CBP aggregation in PhOLEDs with time when under electrical driving, they do not reveal its underlying process. Considering that a similar aggregation phenomenon can be induced by thermal annealing alone, it is natural to wonder if PhOLEDs degradation is simply due to CBP aggregation induced by Joule heating arising from the current flow during device operation.[21] Therefore, to uncover the exact mechanism, we study the degradation behavior of the CBP/TPBi interface under various stress scenarios utilizing hole-only (h-only) devices. The structure of the devices is ITO/MoO_3(5 nm)/CBP(30 nm)/TPBi(10 nm)/

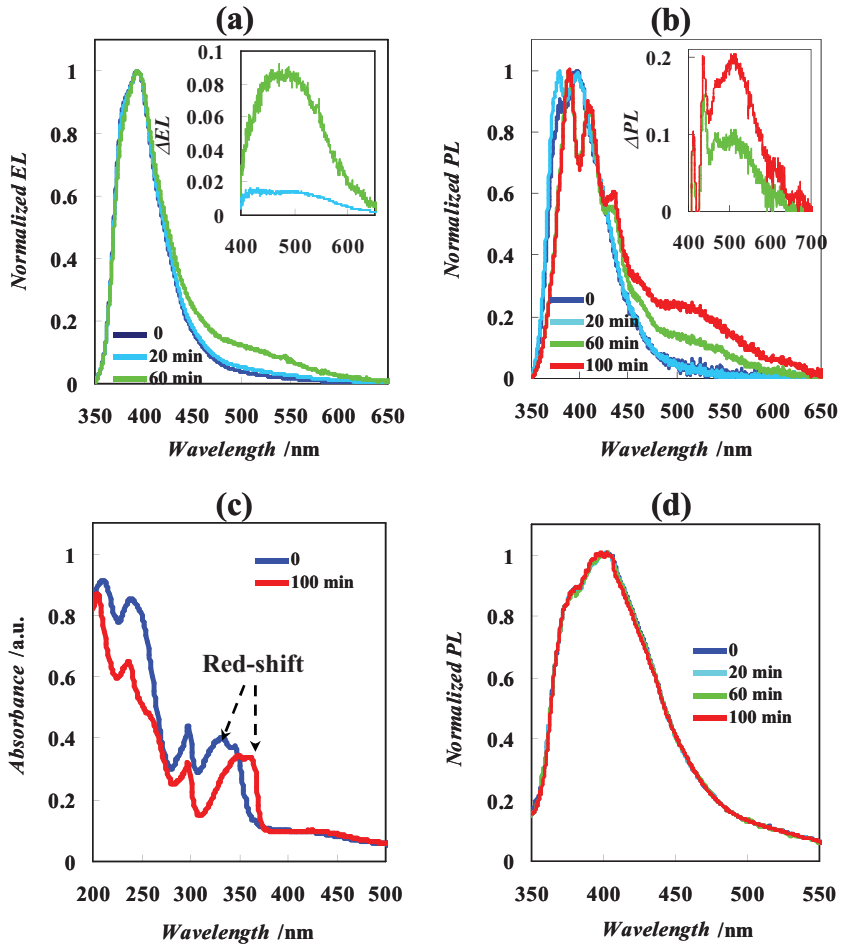

Figure 5. (a) Normalized EL spectra of a device of structure ITO(120 nm)/MoO_3(5 nm)/CBP(40 nm)/TPBi(30 nm)/LiF(0.5 nm)/Al(100 nm) before and after annealing at 120 °C for 20 and 60 min in a N_2 atmosphere. The inset shows the differences between the EL spectra after 20 minutes and 60 minutes of annealing relative to the initial one. (b) Normalized PL spectra under a 365 nm excitation of a CBP film before and after annealing at 120 °C for 20, 60 and 100 min in a N_2 atmosphere. The inset shows the differences between the PL spectra after 60 and 100 min of annealing relative to the initial one. (c) Absorption spectra of a CBP film before and after 100 min of annealing at 120 °C. (d) Normalized PL under a 312 nm excitation of a TPBi film before and after thermal annealing at 150 °C.

MoO_3(10 nm)/Al(100 nm), as shown in **Figure 6**a. When under a forward bias (i.e., the ITO is positively biased relative to the Al), the injection of electrons from the Al is blocked by the top MoO_3, and therefore the flow of current occurs exclusively by holes injected from the ITO. As a result, these devices show h-only transport characteristics.[16] Figure 6b shows the changes in V_d (ΔV) driven by a current of density 20 mA cm^{-2} in these devices versus time, during which the devices are subjected to one of three stress scenarios: (1) Current flow only (denoted by <I only>), under a forward bias to sustain a current flow of density ~20 mA cm^{-2}; (2) Irradiation by light only (denoted by <L only>), at 365 nm of power density ~0.5 mW cm^{-2}; (3) Current flow and irradiation together (denoted by <I + L>), subjected to scenarios (1) and (2) simultaneously. Also, we keep a control device in the dark to be used as a reference (denoted by <C>). The temperature of these devices is maintained at ~22 °C. For comparison, we also include traces representing the algebraic sum of the ΔV values caused by the scenarios <I only> and <L only> (denoted by Σ(<I only>, <L only>)). As Figure 6b shows, the flow of current alone or irradiation alone brings about an increase in the V_d with time, reflected in the ΔV values in the figure, which can be attributed to the hole accumulation at the CBP/TPBi interface [11] and the photo-degradation of the ITO/MoO_3/CBP contact,[15] respectively. What is most significant in the figure, however, is that the measured ΔV values due to the scenario <I + L> are not only much higher than those due to the scenarios <I only> or <L only>, but are also much higher than the corresponding computed Σ(<I only>, <L365nm only>) values (i.e., the sum of the ΔV values due to the scenarios <I only> and <L only>). Such additional increase in V_d exhibited in the scenario <I + L> is essentially indicative of the degradation of the CBP/TPBi interface, and is determined to be due to interactions between CBP excitons and CBP positive polarons in its vicinity.[16]

After ~18 h under the above conditions, we peel off the Al cathodes of the four devices using a scotch tape in a N_2 atmosphere.[22] Since the adhesion of inorganic/inorganic interfaces is much stronger than that of organic/inorganic interfaces,[23] the 10 nm MoO_3 layer would also be peeled off with the Al cathode. We then deposit LiF(1 nm)/Al(100 nm) cathodes on these devices. As now, electron injection from the Al cathode becomes possible, and hence bipolar transport and EL become possible. The process is illustrated in **Figure 7**a, in which these h-only devices are converted to light-emitting devices by cathode replacement. Figure 7b presents the normalized EL spectra of these devices, showing blue EL from CBP. Remarkably, as the inset more clearly illustrates, the device subjected to the scenario <I + L> shows a broader EL spectrum than the devices subjected to the scenarios <I only> and <L only> and kept in the dark. Figure 7c displays the "spectral shift" observed in the devices subjected to the scenarios <I + L>, <I only> and <L only>, obtained from the mathematical difference in the EL spectra of the three devices after the aging relative to the control one. As Figure 7c shows, only the device subjected to the scenario <I + L> shows a significant change in the EL spectrum relative to the control one, and the difference corresponds to a band with peak at ~500 nm. Given the obvious similarity between this band and the corresponding one in Figures 3 to 5, we can ascribe it to the formation of CBP aggregates. The difference in the spectra of the device subjected to the scenario <I + L> and those subjected to <I only> or <L only> rules out the possibility that the aggregation may be due to Joule heating, and indicate that it must be due to the co-existence of both CBP excitons and CBP

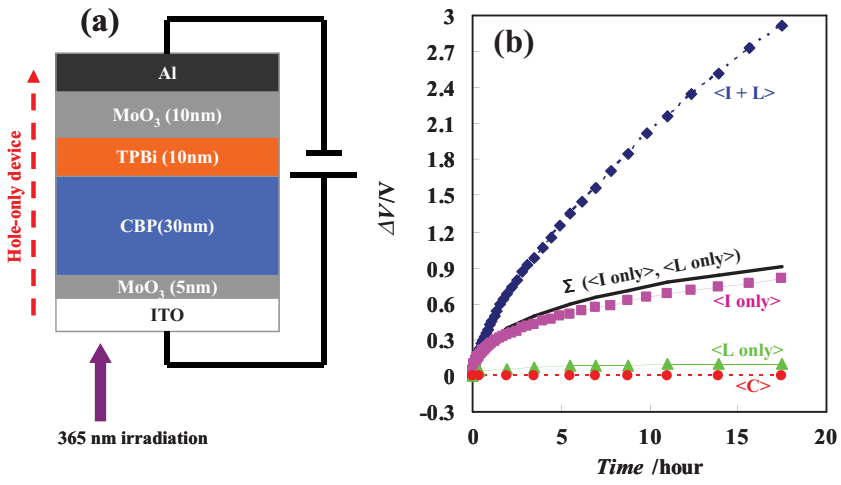

Figure 6. (a) H-only devices of structure ITO/MoO_3(5 nm)/CBP(30 nm)/TPBi(10 nm)/MoO_3(10 nm)/Al(100 nm). (b) Changes in V_d (ΔV) driven by a current of density 20 mA cm^{-2} in the devices versus time, during which these devices are subjected to scenarios <I only>, <L only> and <I + L> and kept in the dark (i.e., <C>). Traces representing the algebraic sum of the ΔV values caused by the scenarios <I only> and <L only> (denoted by Σ(<I only>, <L only>)) is also included.

positive polarons (i.e., due to exciton–polaron interactions). This shows that exciton-polaron interactions can induce aggregation in CBP, similar to that induced by thermal annealing. Given the fact that both CBP excitons and CBP positive polarons are present simultaneously in high concentrations in the e-h recombination zone (i.e., the vicinity of the CBP/TPBi interface) in PhOLEDs during normal operation, the same effect can take place. Thus, we may conclude that the changes in the EL spectra of PhOLEDs with electrical driving time observed in Figures 3 and 4 are the result of CBP aggregation in the recombination zone due to exciton-polaron interactions. Since this aggregation process is triggered by the co-existence of both excitons and positive polarons, but not by the presence of excitons or polarons separately, it is exciton-polaron-induced aggregation (EPIA) in nature. It should be pointed out that the co-existence of excitons and negative polarons

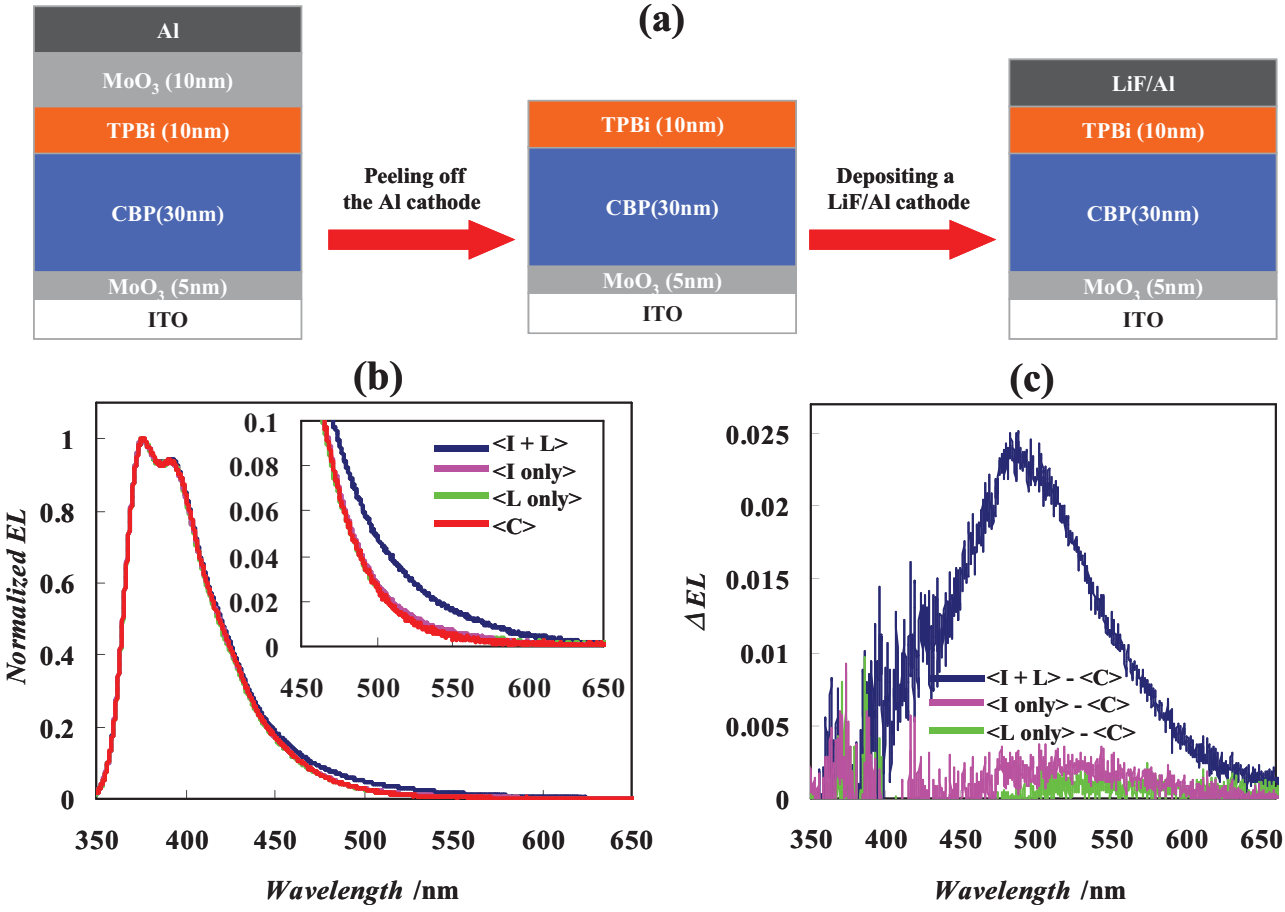

Figure 7. (a) Illustration of the cathode replacing process, in which h-only devices are converted to light-emitting devices. (b) Normalized EL spectra of the four light-emitting devices. The inset shows a detailed view of the spectra at ~500 nm. (c) Differences between the EL spectra of the devices subjected to the scenarios <I + L>, <I only> and <L only> relative to that of the control device.

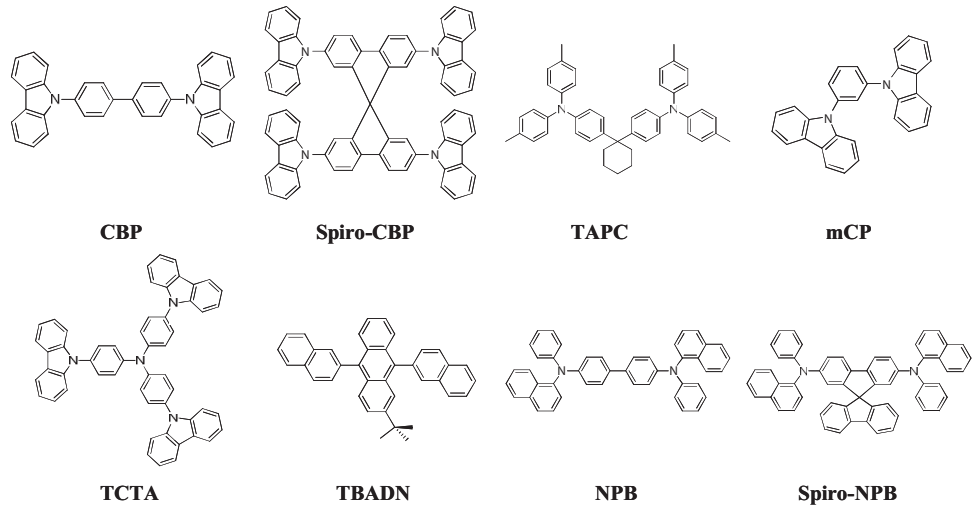

Figure 8. Molecular structures of a range of organic materials.

on CBP does not lead to a similar EPIA effect, since only positive polarons were found to interact with excitons and lead to the observed degradation whereas negative polarons were not.[16] This exactly corresponds to the scenario in PhOLEDs during operation where the CBP polarons that accumulate in the vicinity of the CBP/TPBi interface are mostly positive.[3]

Finding CBP aggregation due to exciton-polaron interactions, we can describe the underlying mechanism by the following two-step general scheme:

$$M_+ + M^* \rightarrow M_+^* + M \quad (1)$$

$$M_+^* + M(or\ M_+^* + M_+^*) \rightarrow D \quad (2)$$

where M^+ represents positive polarons on CBP monomers, M^* represents excitons of CBP monomers, M^*_+ represents excited positive polarons on CBP monomers (i.e., excited CBP cations), M represents CBP monomers in the ground state and D represents CBP aggregate species (e.g., a dimer) in the ground state. When a PhOLED is driven by a current, both CBP positive polarons and CBP excitons will co-exist in high concentrations in the vicinity of the CBP/TPBi interface. An energy transfer between these two species can lead to the formation of a CBP excited positive polaron state, described in step (i). Since this state has an electron in a high energy level (i.e., the lowest unoccupied molecular orbital (LUMO)) and at the same time has an unoccupied highest occupied molecular orbital (HOMO), it can be expected to be particularly prone to intermolecular aggregation in order to reach a more energetically favorable state, described in step (ii). These CBP aggregates will have narrower bandgap than their monomer precursors and produce EL at longer wavelength. They will also be capable of trapping charges and quenching excitons, and thus lead to an increase in V_d and a decrease in EL efficiency, which are all common observations associated with PhOLEDs degradation. As the EPIA process takes place mainly in the vicinity of the CBP/TPBi interface (where most e-h recombination and EL originates in PhOLEDs), this degradation mechanism occurs primarily at the interface.

In order to verify that these changes are morphological in nature, and to rule out chemical degradation, we use NMR spectroscopy to analyze the molecular structure of CBP aggregates. The experimental details and data are provided in detail in the supplementary material section. The NMR results show no detectable changes in the chemical fingerprint of CBP when subjected to electrical driving, verifying that the degradation mechanism is exclusively morphological (i.e., aggregation) in nature.

2.4. Exciton–Polaron-Induced Aggregation in Other Wide-Bandgap Materials

Uncovering EPIA in CBP, it becomes interesting to see if the same phenomenon occurs in other materials. We therefore conduct similar studies on a range of materials, some of which are commonly used as hosts in PhOLEDs. These materials are 2,2′,7,7′,-tetrakis(carbazol-9-yl)-9,9-spirobifluorene (Spiro-CBP), 1,1′-bis(di-4-tolylaminophenyl) cyclohexane (TAPC), 1,3-bis(carbazol-9-yl)benzene (mCP), 4,4′,4″-tris(carbazol-9-yl) triphenylamine (TCTA), 9,10-bis(2-naphthyl)-2-t-butyl anthracene (TBADN), *N,N*′-bis (naphthalen-1-yl)-*N,N*′-bis(phenyl) benzidine (NPB) and *N,N*′-bis(naphthalene-1-yl)-*N,N*′-bis(phenyl)-2,7-diamino-9,9-spirobifluorene (Spiro-NPB), and their molecular structures are shown in **Figure 8** (CBP is also included for comparison). **Figure 9**a–e show EL spectra (without normalization) with continuous electrical driving at 20 mA cm^{-2} in devices of general structure ITO/MoO_3(5 nm)/X(30 nm)/TPBi(30 nm)/LiF(0.5 nm)/Al(100 nm), where X is CBP, Spiro-CBP, TAPC, mCP or TCTA. As can be seen from the figures, the EL spectra of all devices change gradually upon electrical driving, all displaying a decrease in intensity of the monomer emission peak, and the emergence of a new band at longer wavelength which can be attributed to the formation of aggregate species of these materials. Clearly, all materials are susceptible to aggregation by exciton-polaron interactions, similar to CBP, but in various extents. As all these materials have wide bandgap (>3.3 eV), a typical request of HMs in PhOLEDs, we also test

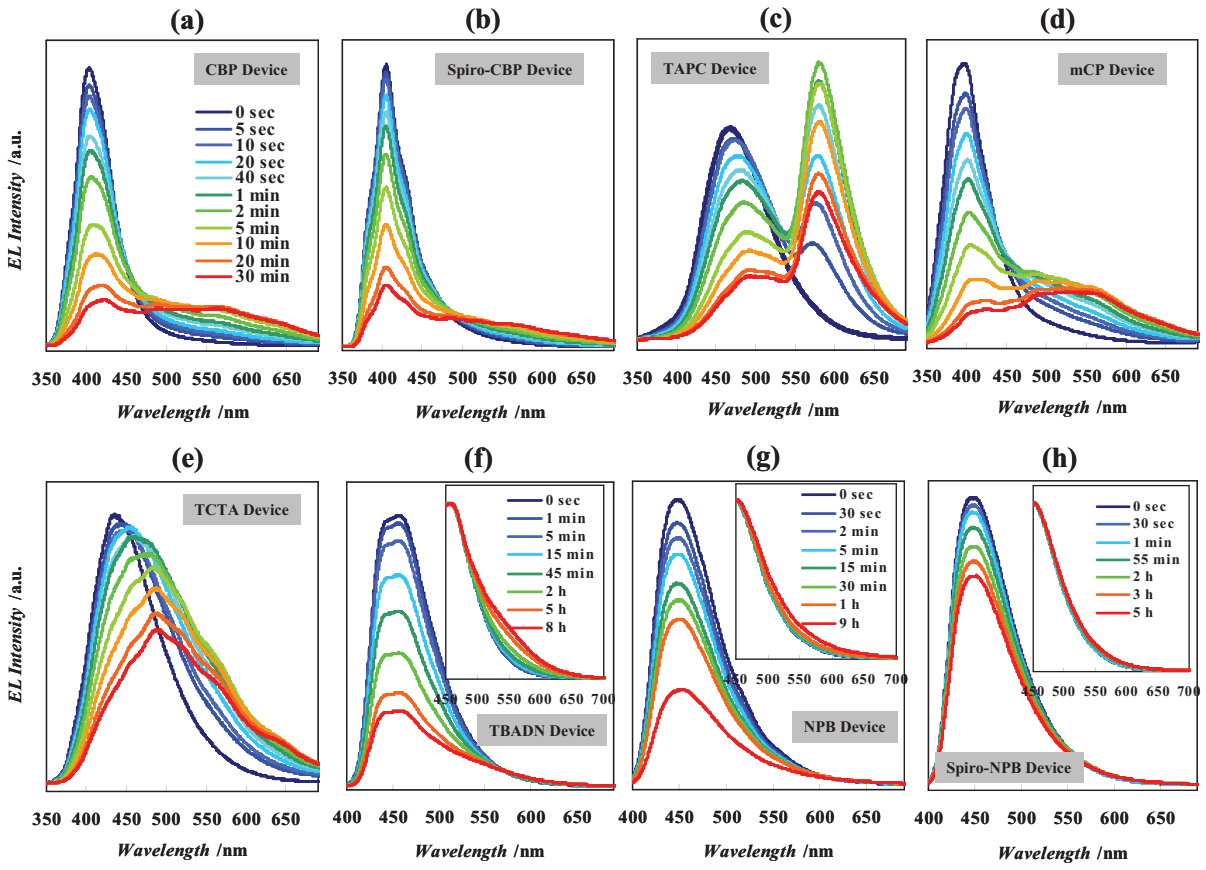

Figure 9. EL spectra (without normalization) with continuous electrical driving at 20 mA cm^{-2} in devices of general structure ITO/MoO_3(5 nm)/X(30 nm)/TPBi(30 nm)/LiF(0.5 nm)/Al(100 nm), where X is CBP, Spiro-CBP, TAPC, mCP, TCTA, TBAND, NPB or Spiro-NPB.

materials with relatively narrower bandgap for comparison. Figure 9f–h show EL spectra (without normalization) with continuous electrical driving of devices with the same structure but with TBADN, NPB and Spiro-NPB, respectively. The normalized EL spectra are illustrated in the insets. Clearly, the extent of aggregation even after much longer periods of electrical driving time is much less in comparison to that in the wide-bandgap materials.

Figure 10a depicts the extent of EPIA in the above materials (defined as the ratio of aggregate emission band intensity to monomer emission band intensity in the EL spectra after 30 min of electrical driving) versus their bandgap (i.e., E_g) (taken from the literature).[3,4,17,24–26] As the figure shows, there is a clear correlation between the extent of aggregation and E_g, where the wide-bandgap materials (such as TAPC, mCP TCTA, CBP and Spiro-CBP) tend to aggregate more significantly in comparison to the narrow-bandgap ones (such as TBADN, NPB and Spiro-NPB). This can be attributed to the fact that in wide-bandgap materials exctions involved in exciton-polaron interactions have higher energy, and thus can induce aggregation more efficiently (e.g., excited polaron species will be more energetic). Quite interestingly, there seems to be a threshold E_g value of ~3.1 eV. When below the threshold, the materials aggregation occurs slowly, whereas when above it, the materials aggregation occurs significantly (with the aggregate to monomer EL bands ratio at least one order of magnitude higher). Surprisingly, there seems to be no correlation between the ease of aggregation and the materials glass-transition (T_g) temperatures (taken from the literature,[27–33] as shown in Figure 10b. This again points to the fact that the root cause of this aggregation in PhOLEDs during electrical driving is fundamentally different and is not simply Joule heating.

These findings uncover a new degradation mechanism based on EPIA of organic materials that severely affects wide-bandgap materials. As PhOLEDs generally use wide-bandgap hosts, this may explain the generally lower stability of PhOLEDs relative to their fluorescent counterparts.

3. Conclusions

We have studied the degradation mechanisms of PhOLEDs. Contrary to expectations, we find that PhOLEDs degradation is not induced by guest excitons, but is related to the presence of host excitons that causes device degradation via exciton-polaron interactions. We determine that the degradation arises from HMs aggregation in the vicinity of EML/ETL interfaces. Further study reveals that such aggregation process is induced by the co-existence of both excitons and positive polarons on HMs. Such aggregation process is found to occur in a

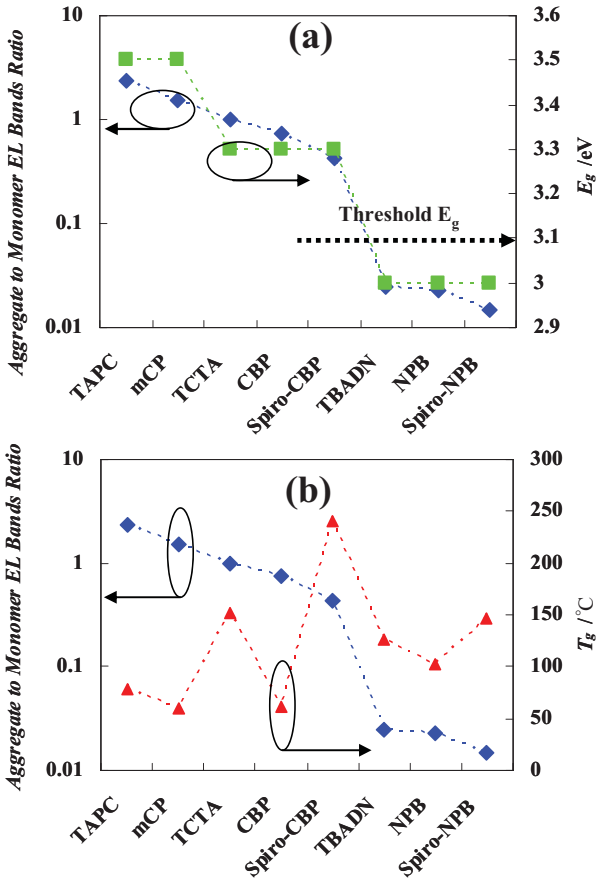

Figure 10. Ratio of aggregate/monomer EL bands versus the materials (a) E_g and (b) T_g temperatures.

variety of wide-bandgap materials commonly used as hosts in PhOLEDs and is correlated with device degradation. Quite notably, the extent of aggregation appears to correlate with the materials bandgap rather than with their T_g temperatures. The findings uncover a significant degradation mechanism in PhOLEDs that is exciton–polaron-induced and interfacial in nature. Although this study has focused on PhOLEDs, we can expect the same degradation mechanism to affect other organic optoelectronic devices such as organic solar cells and organic photodetectors.

4. Experimental Section

In this work, PhOLEDs of the "simplified" architecture[3] made of typical organic materials are fabricated and tested. In these devices, a variety of wide-bandgap materials including CBP, Spiro-CBP, TAPC, mCP, TCTA, TBADN, NPB and Spiro-NPB are used as both hole-transport layers and emitter hosts, whereas TPBi is used as an ETL. $Ir(ppy)_3$ and PtOEP are used as phosphorescent guests doped into HMs. ITO and Al are used as anode and cathode, respectively. All the devices are fabricated by the vacuum deposition of organic materials and metals at a rate of 1 Å s^{-1} at a base pressure of about 5×10^{-6} Torr on CF_4/O_2 plasma-cleaned[14] ITO-coated (~120 nm thick) glass substrates. Monochromatic illumination from a 200 W Hg-Xe lamp equipped with an Oriel-77200 monochromator is used for irradiation tests and photoluminescence measurements. An Edinburgh Instruments FL920 spectrometer is used for time domain fluorescence lifetime measurements. All tests are carried out in a N_2 atmosphere.

Supporting Information

Supporting Information is available from the Wiley Online Library or from the author.

Acknowledgements

Financial support to this work by Teledyne-DALSA and the Natural Science and Engineering Research Council of Canada (NSERC) is gratefully acknowledged. QW also acknowledges financial support from the Ontario Graduate Scholarship (OGS).

Received: November 12, 2013
Revised: December 1, 2013
Published online: January 29, 2014

[1] M. A. Baldo, D. F. O'Brien, Y. You, A. Shoustikov, S. Sibley, M. E. Thompson, S. R. Forrest, *Nature* **1998**, *395*, 151.
[2] S. Reineke, T. C. Rosenow, B. Lussem, K. Leo, *Adv. Mater.* **2010**, *22*, 3189.
[3] M. G. Helander, Z. B. Wang, J. Qiu, M. T. Greiner, D. P. Puzzo, Z. W. Liu, Z. H. Lu, *Science* **2011**, *332*, 944.
[4] Z. B. Wang, M. G. Helander, J. Qiu, D. P. Puzzo, M. T. Greiner, Z. W. Liu, Z. H. Lu, *Appl. Phys. Lett.* **2011**, *98*, 073310.
[5] Z. B. Wang, M. G. Helander, J. Qiu, D. P. Puzzo, M. T. Greiner, Z. M. Hudson, S. Wang, Z. W. Liu, Z. H. Lu, *Nat. Photonics* **2011**, *5*, 753.
[6] C.-H. Gao, S.-D. Cai, W. Gu, D.-Y. Zhou, Z.-K. Wang, L.-S. Liao, *Appl. Mater. Interfaces* **2012**, *4*, 5211–5216.
[7] N. C. Giebink, B. W. D'Andrade, M. S. Weaver, P. B. Mackenzie, J. J. Brown, M. E. Thompson, S. R. Forrest, *J. Appl. Phys.* **2008**, *103*, 044509.
[8] N. C. Giebink, B. W. D'Andrade, M. S. Weaver, J. J. Brown, S. R. Forrest, *J. Appl. Phys.* **2009**, *105*, 124514.
[9] D. Y. Kondakov, W. C. Lenhart, W. F. Nichols, *J. Appl. Phys.* **2007**, *101*, 024512.
[10] S. Scholz, K. Walzer, K. Leo, *Adv. Funct. Mater.* **2008**, *18*, 2541–2547.
[11] H. Siboni, H. Aziz, *Appl. Phys. Lett.* **2012**, *101*, 173502.
[12] H. Siboni, H. Aziz, *Org. Electron.* **2011**, *12*, 2056–2060.
[13] H. Siboni, Y. Luo, H. Aziz, *J. Appl. Phys.* **2011**, *109*, 044501.
[14] Q. Wang, G. Williams, H. Aziz, *Org. Electron.* **2012**, *13*, 2075–2082.
[15] Y. Zhang, M. A. Abdelmalek, Q. Wang, H. Aziz, *Appl. Phys. Lett.* **2013**, *103*, 063307.
[16] Q. Wang, H. Aziz, *Appl. Mater. Interfaces* **2013**, *5*, 8733–8739.
[17] Q. Wang, Y. Luo, H. Aziz, *J. Appl. Phys.* **2010**, *107*, 084506.
[18] R. C. Kwong, M. R. Nugent, L. Michalski, T. Ngo, K. Rajan, Y.-J. Tung, M. S. Weaver, T. X. Zhou, M. Hack, M. E. Thompson, S. R. Forrest, J. J. Brown, *Appl. Phys. Lett.* **2002**, *81*, 1.
[19] J. M. Lupton, *Appl. Phys. Lett.* **2002**, *81*, 2478–2480.
[20] H. Bassler, *Phys. Stat. Sol. B* **1981**, *107*, 9.
[21] J.-R. Gong, L.-J. Wang, S.-B. Lei, C.-L. Bai, X.-H. Zhang, S.-T. Lee, *J. Phys. Chem.* **2005**, *109*, 1675–1682.
[22] Q. Wang, Y. Luo, H. Aziz, *Appl. Phys. Lett.* **2010**, *97*, 063309.
[23] T. Tong, B. Babatope, S. Admassie, J. Meng, O. Akwogu, W. Akande, W. O. Soboyejo, *J. Appl. Phys.* **2009**, *106*, 083708.

[24] S. Yang, M. Jiang, *Chem. Phys. Lett.* **2009**, *484*, 54–58.
[25] H. Kanno, R. J. Holmes, Y. Sun, S. Kena-Cohen, S. R. Forrest, *Adv. Mater.* **2006**, *18*, 339–342.
[26] S. H. Kim, J. Jang, J. Y. Lee, *Appl. Phys. Lett.* **2007**, *91*, 083511.
[27] X. Yang, H. Huang, B. Pan, M. P. Aldred, S. Zhuang, L. Wang, J. Chen, D. Ma, *J. Phys. Chem. C* **2012**, *116*, 15041–15047.
[28] M.-H. Tsai, Y.-H. Hong, C.-H. Chang, H.-C. Su, C.-C. Wu, A. Matoliukstyte, J. Simokaitiene, S. Grigalevicius, J. V. Grazulevicius, C.-P. Hsu, *Adv. Mater.* **2007**, *19*, 862–866.
[29] H.-C. Yeh, H.-F. Mengb, H.-W. Lin, T.-C. Chao, M.-R. Tseng, H.-W. Zan, *Org. Electron.* **2012**, *13*, 914–918.
[30] T. Saragi, T. Fuhrmann-Lieker, J. Salbeck, *Adv. Funct. Mater.* **2006**, *16*, 966–974.
[31] T. Spehr, R. Pudzich, T. Fuhrmann, J. Salbeck, *Org. Electron.* **2003**, *4*, 61–69.
[32] Y.-C. Tsai, J.-H. Jou, *Appl. Phys. Lett.* **2006**, *89*, 243521.
[33] J. Y. Shen, C. Y. Lee, T.-H. Huang, J. T. Lin, Y.-T. Tao, C.-H. Chien, C. Tsai, *J. Mater. Chem.* **2005**, *15*, 2455–2463.